Ultralow power trapping and fluorescence detection of single particles on an optofluidic chip†

S. Kühn,[a] B. S. Phillips,[b] E. J. Lunt,[b] A. R. Hawkins[b] and H. Schmidt*[a]

Received 4th August 2009, Accepted 2nd October 2009
First published as an Advance Article on the web 16th November 2009
DOI: 10.1039/b915750f

The development of on-chip methods to manipulate particles is receiving rapidly increasing attention. All-optical traps offer numerous advantages, but are plagued by large required power levels on the order of hundreds of milliwatts and the inability to act exclusively on individual particles. Here, we demonstrate a fully integrated electro-optical trap for single particles with optical excitation power levels that are five orders of magnitude lower than in conventional optical force traps. The trap is based on spatio-temporal light modulation that is implemented using networks of antiresonant reflecting optical waveguides. We demonstrate the combination of on-chip trapping and fluorescence detection of single microorganisms by studying the photobleaching dynamics of stained DNA in E. coli bacteria. The favorable size scaling facilitates the trapping of single nanoparticles on integrated optofluidic chips.

Introduction

Holding an object up to regard its workings is probably the original act of analytical science. While macroscopic objects are handled with ease, the diffusive motion of microscopic objects necessitates fundamentally different means of manipulation. Among these, optical force traps and laser tweezers[1,2] have become a mainstay in biology, molecular biology, immunology, and other related fields. They allow for the non-invasive capture and manipulation of microscale objects over extended periods of time with an accuracy that can reach the angstrom level. Despite their advantages and conceptual elegance, optical force traps and tweezers have some shortcomings. They typically require high optical powers of tens to hundreds of milliwatts, especially for smaller particles or biological objects with low index contrast to the surrounding medium. This can result in the inability to trap small particles and creates the danger of damaging the object under study.[3] Techniques to enhance the optical field locally[4] or to optically trigger a local electrical force[5] have been developed for microfluidic microscopy to drastically reduce the optical power levels. An active trapping scheme as proposed by Enderlein[6] can make do with similarly low optical excitation powers. In this case, the position of a fluorescent particle is detected optically, but the restoring force that compensates the particle's movement away from the trapping point is provided by other means.[7–9] Another problem that has hampered commercial use of optical force traps is the need for high-end microscopy equipment and skills to build and operate the trapping apparatus. This issue can now be addressed using on-chip optical force traps. To date, this approach still requires very high optical powers.[10–12]

We present a solution to these problems that allows for prolonged observation and analysis of sub-microscopic objects by using active electro-optical trapping on an optofluidic chip. It features operation at ultralow optical power, compatibility with simultaneous ultra-sensitive optical detection, absence of fundamental limits for particle size or refractive index, and highly efficient utilization of analyte solution. By implementing waveguide-based optical feedback on a planar optofluidic chip, we demonstrate a reduction in trapping power by 5 orders of magnitude compared to conventional optical force traps. Simultaneous manipulation (trapping) and optical studies of single particles are enabled by integrated waveguides in a planar optofluidic setting. Specifically, individual polystyrene microbeads in solution can be loaded one by one into an interrogation volume of ~100 femtoliters and optically analyzed for several minutes or longer. We illustrate the applicability to biological problems by measuring the dynamics of the photobleaching process of stained DNA in single E. coli bacteria. We also describe the benefits of additional confinement perpendicular to the fluidic channel on trapping efficiency and scaling with trapped particle size. The demonstrated properties of the new trap overcome limitations of current all-optical techniques and open perspectives for automated single object analysis in healthcare, environmental and other analytic applications.

Experimental

Trap architecture and working principle

The new integrated active trap is implemented on an optofluidic platform that utilizes hollow, AntiResonant Reflecting Optical Waveguides (ARROWs) to confine light and liquids in the same volume over length ranges on the order of centimetres.[13] ARROW structures represent dielectric reflecting enclosures that enable light guiding in a medium with an index lower than the

[a]*School of Engineering, University of CA Santa Cruz, Santa Cruz, CA, 95064, USA. E-mail: hschmidt@soe.ucsc.edu; Fax: +1 831-459-4829; Tel: +1 831-459-1482*
[b]*ECEn Department, Brigham Young University, Provo, UT, 84602, USA*

† Electronic supplementary information (ESI) available: Additional data and explanations on the micro-fabrication parameters of the ARROW and on the analysis of the trap, and description of the supplementary movies. Movie S1: "capture of a 1 μm fluorescent latex bead in the electro-optical trap", movie S2: "single particle trapping in presence of multiple microbeads" and movie S3: "fluorescence from DNA of a trapped E. coli bacterium". See DOI: 10.1039/b915750f

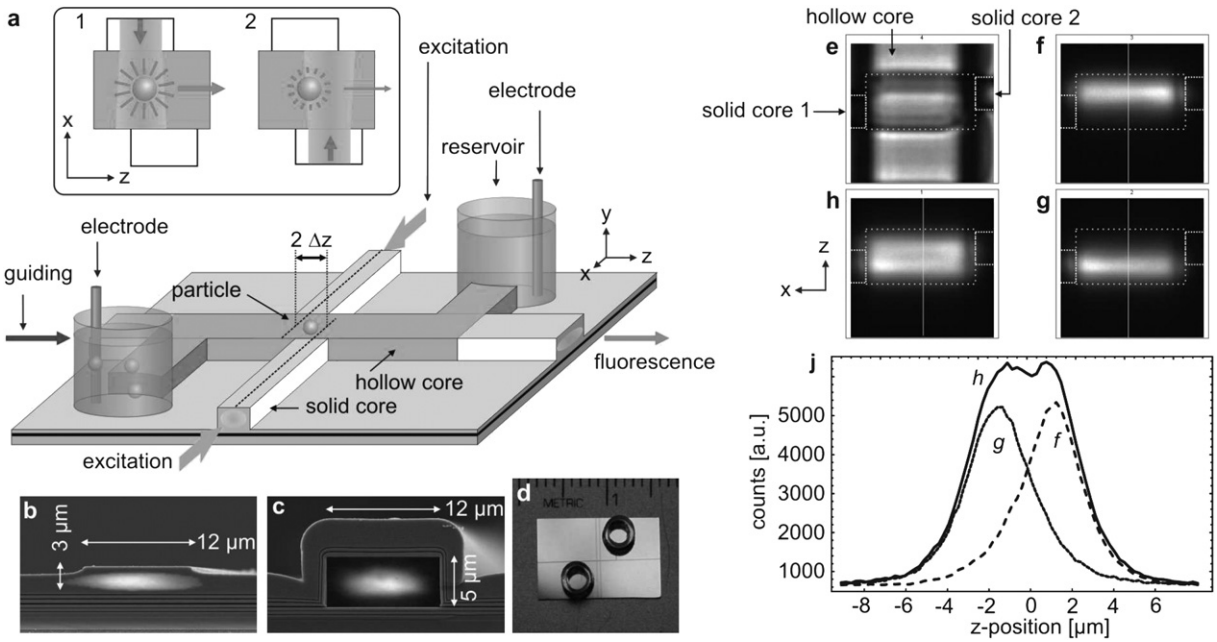

Fig. 1 (a) Schematic layout of the ARROW optofluidic analysis platform. Inset: Working principle of the particle position sensor showing the illumination during 1) the first and 2) the second half-period of modulation. (b) Solid-core waveguide with overlayed optical mode profile. (c) Same for hollow-core waveguide. (d) Photograph of the actual chip with reservoirs. (e) Bright-field top view of the intersection region with boundary outline. (f–h) Fluorescence micrographs of the excitation beams with the right, left and both beams activated. (j) Cross-section as indicated in f–h.

surrounding material. Light can be routed to and from the hollow waveguide along standard ridge waveguides. These are also used to define local excitation volumes at waveguide intersections on the order of 100 fl. The overall chip layout along with the waveguide dimensions of the sample used in this study are shown in Fig. 1a–d.

The waveguide walls provide a natural means for confinement in x and y, but particles inside the hollow waveguide are free to move along z. The main concern is, therefore, to counteract any longitudinal motion that limits typical observation times to a fraction of a second. This motion can result from drift (*e.g.* residual pressure flow) or simply from diffusion (Brownian motion).

The optofluidic electro-optical trap is rooted in Enderlein's active tracking and freedback approach. Its working principle can be summarized as follows. A fluorescent particle is excited by two periodically alternating, spatially distinct beams, and sends out a modulated signal to a detector. For this purpose, an asymmetric waveguide intersection was defined as shown in Fig. 1a. The two solid-core waveguides on either side of the liquid core are slightly offset by $2\Delta z$ and define two overlapping excitation volumes that can be selectively addressed by pump fibers from either side of the chip. The counts of both beams are compared to locate the particle in the illumination pattern. A particle residing at the center of the intersection experiences equal excitation rates from both beams. If the particle drifts or diffuses along z, this balance will be disturbed and thus the difference in the fluorescence counts between the two beams provides magnitude and direction of the excursion. To visualize the excitation volumes in this arrangement, the liquid core was filled with a fluorescent dye solution and imaged with a CCD camera. As can be seen in Fig. 1f–j, the profiles of the two beams resemble two Gaussian functions that intersect at their points of steepest decent, *i.e.* at half the beam waist w_z. This choice of offset maximizes the gradient in the position signal, keeps the total illuminated volume small and the particle excitation efficiency high to avoid a deterioration of the signal-to-background ratio.

In a second step, a corrective force is applied to drive the particle towards the equilibrium position, where both beams have the same intensity. This feedback actuation is implemented through electrokinetic forces. To this end, voltages between 1 and 100 V are applied across the fluidic channel using electrodes immersed in the reservoirs. Embedding the electro-optical trap into an optically and fluidically planar architecture has the advantage over earlier implementations of such traps of the excitation and trapping regions being precisely defined during the fabrication process and not during operation of the trap. This makes the trap easy to set up and use.

Optofluidic chip design

Hollow-core ARROW waveguides were built on a silicon substrate with a previously described process,[14] combining plasma-enhanced chemical vapor deposition of dielectric layers (SiO_2: $n = 1.475$ and SiN: $n = 2.05$, layer sequence: see ESI)† and patterning of a sacrificial core layer (SU-8 3005, Microchem). Solid-core waveguides were formed by contact photolithography (MA150, Karl Suss America) and a 1 μm-deep reactive ion etch (Anelva Corp.) under CF_4. The ends of the SU-8 core were exposed by reactive ion etch. Nanostrip acid (Rockwood Electronic Materials) was used to remove SU-8 from the hollow channel. Metal cylinders glued over the open ends served as fluid reservoirs. Light from single-mode fibers was end-to-end coupled

to the chip. The design included an adiabatically tapered section in the solid-core waveguides to laterally expand the fiber mode of about 4 μm full width at half maximum (FWHM) to 9 μm FWHM in the hollow waveguide. This design efficiently suppresses mode beating and ensures a well defined transverse profile of the guiding beam for the present experiments.

Electro-optic trap design

A chopper wheel was arranged to alternatingly block the light launched into the two excitation waveguides, typically at a rate of 1 kHz. Fluorescence light emitted by a particle is guided by the liquid core, collected from a merging solid core waveguide and detected by an APD. Signal processing was based on a simple lock-in amplifier,[15] an 8 bit digital-to-analog converter and a low power high-voltage amplifier. Electrokinetic feedback actuation[16] was applied through silver-chloride electrodes (Fig. 1a). The particle motion can result from electophoresis, electroosmosis, or a combination. For stable and reproducible trapping, however, the charge states of the particles and the solution had to be controlled. For excitation we used an Nd:YAG laser (532 nm) or a HeNe laser (633 nm), while the guiding beam was provided by a Ti:Sapphire laser (Coherent MIRA 900F, operated at 820 nm). All experiments were monitored using a home-built microscope (Olympus, ULWD, NA 0.45, 50x) equipped with a cooled high sensitivity CCD camera (Andor Tech., Luca).

Bead and bacteria solutions

Fluorescent microbeads and nanobeads (diameters 1 μm and 200 nm, Tetraspeck, Invitrogen) were diluted in ultrapure water at 1 : 100 and 1 : 1000 with the addition of 0.1% Triton X to avoid wall adhesion.

Escherichia coli bacteria (strain: K12-D21, Genetic Stock Center, Yale University) were grown overnight and washed twice in ultrapure water to remove any residual growth medium. They were stained with SYTO 82 (5 μM solution, Invitrogen) for 30 min and subsequently washed once more to separate unbound dye. 1% of the polymer POP 4 (Invitrogen) was added to the solution to suppress electroosmosis. Initial studies showed that this dynamic coating of the channel walls with this polymer leads to a well defined electrokinetic response. The electrophoretic mobilities were determined by observing the particle motion under a square wave voltage along the channel. A linear voltage drop along the 8 mm liquid channel was assumed.

Results and discussion

Low-power trapping of single microbeads

To prove the functionality of the trap, we injected a solution of 1 μm microbeads into the channel. The highest velocity v_{max} that the feedback must be able to impose on the particle is related to the dimensions of the trapping region $2\Delta z \approx w_z \approx 2$ μm and the particle diffusion coefficient $D \approx 0.5$ μm^2 s^{-1} by $v_{max} \geq D/\Delta z$. With an electrokinetic mobility of $\mu_e \approx 5.4 \times 10^{-2}$ μm s^{-1} m V^{-1}, trapping can be achieved at voltages around 1 Volt. Ultra-low pump powers in the 1 μW range ($\lambda_{ex} = 632$ nm) as measured at the output of the fibers were sufficient to operate the trap. Since some of this power is lost between the input facet of the chip and the liquid channel (solid-core waveguide loss of $\alpha_s \approx 0.67$/cm; fiber to waveguide coupling efficiency of $\kappa \approx 55\%$), we estimate an excitation power at the bead of only 0.4 μW. This is up to 5 orders of magnitude less than previously used in on-chip optical force traps for particles of similar or even larger size.[10,17,12] In Fig. 2a, we show a combined fluorescence and bright-field image of a trapped particle that also reveals the physical structure of the waveguide system. The trajectory of the particle is recorded by an imaging CCD camera. As shown in the position histogram (Fig. 2b), the bead's motion is observed in a region below ±1 μm in z within the detection region. A detailed analysis of the recorded images‡ allows to estimate the mean square deviation reaching down to ±200 nm. Since the trapped particle resides in the linear feedback regime, the standard deviation can be related to an effective spring constant of $k_z \approx 90$ nN/m.[18] Normalized with respect to power and particle volume, this stiffness is approximately 35 to 140 times higher than for optical near-field traps.[4,11] In this instance, the particle remained trapped for more than one minute (the complete trapping process is shown in movie S1 in the ESI).† Residence time intervals in the waveguide intersection on the order of several tens of seconds were typical. This constitutes an improvement by more than two orders of magnitude compared to free diffusive motion or gradient-driven particle flow. Large-amplitude conformational changes, protein folding and structural reorganizations, and complex formation are examples of biomolecular processes that evolve at these timescales and thus can be monitored with this trap.

The fluctuations of the fluorescence signal detected during trapping along the waveguide by the APD are shown in Fig. 2c. They arise from diffusion through the spatially limited excitation-detection volume and may be used to determine the diffusion properties by fluctuation correlation spectroscopy (FCS) analysis.[19] It is a virtue of active trapping that positional fluctuations are transferred from the fluorescence signal to the feedback force parameter, thereby extending the useful FCS bandwidth. A more thorough account of FCS under tracking control is given in ref. 20.

An important intrinsic advantage of the active trap is that it does not accumulate particles as optical traps would, instead ensuring the observation of a single particle at a time. Since the (diffusive) motion of individual particles is uncorrelated, the feedback mechanism compensates only the movements of the particle that resides in the trap.[21] Thus, the electric feedback signal does not result in directed motion for other particles even though they are subjected to the electrokinetic force. This feature is illustrated in movie S2 in the ESI† which shows two microbeads in the waveguide channel. Once one of the particles enters the active trapping region, it remains stably trapped around the center of the channel while the second particle undergoes uncorrelated movements away from the trapping region. As long as the particle concentration is not

‡ The peak at ~6 μm arises from an optical distortion of the bead's fluorescence image observed through the CCD microscope by the waveguide edges. The position information obtained from these specific images, therefore, does not represent the true particle position but shows excessive excursions toward the left. If these artefacts are removed, the particle histogram shows only a single peak at ~7 μm and a lower limit of 200 nm is found for the mean square particle deviation.

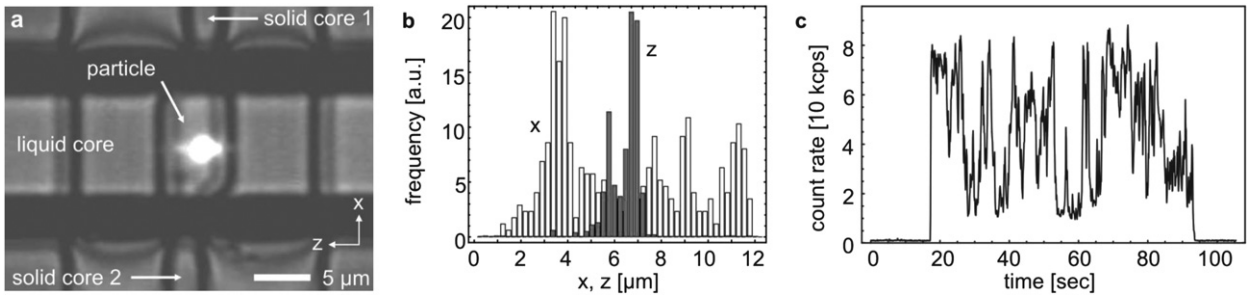

Fig. 2 (a) Bright-field and fluorescence image of a trapped 1 μm bead. (b) Position histograms for the particle x (empty bars) and z location (filled bars). (c) Time trace of the corresponding APD fluorescence signal.

high enough to cause repeated random entries by other particles into the intersection region, the device acts as a true single-particle trap.

Fluorescence studies of trapped E. coli bacteria

The ultralow optical excitation power levels required for position sensing allow us to use the same beam for both trapping and fluorescence studies of a single particle using exclusively optical waveguides. In order to demonstrate the application of this main feature to bio-analysis, we studied the DNA fluorescence dynamics in Escherichia coli bacteria (E. coli). To produce a fluorescence signal, the DNA in the bacteria's nuclei were stained with an intercalating dye as described above. Fig. 3a shows the x-z trajectory of an E. coli bacterium trapped for 20 s with an excitation power of only a few microwatts and confined within ±200 nm along the fluidic channel (Fig. 3b). This confinement corresponds to a trap stiffness of $k_z \approx 91$ nN/m as obtained from a Gaussian fit (see Fig. 3b). The lower electrokinetic mobility of E. coli in pure water requires elevated actuation voltages on the order of ±90 Volts.

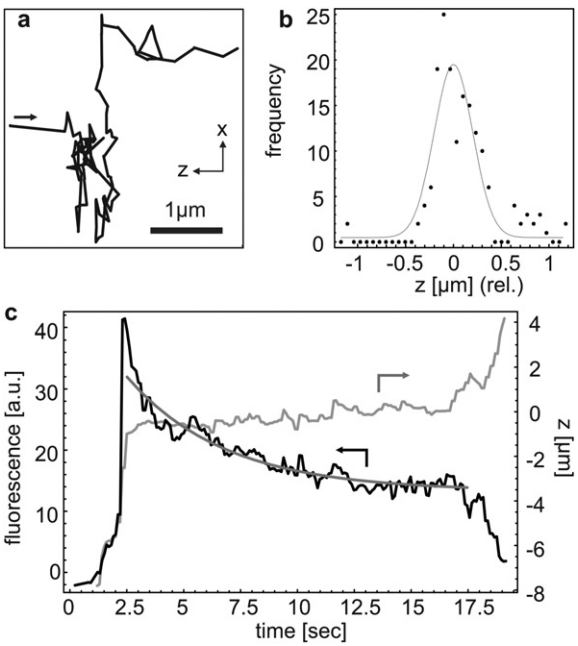

Fig. 3 (a) Time-dependent x–z trajectory of E. coli bacterium showing effective trapping along the channel direction. (b) Position histograms for the bacterium's z location with Gaussian fit showing trapping with a standard deviation of 203 nm. (c) Time traces of the fluorescence signal and the z-position of a single trapped E. coli bacterium during gradual photobleaching. The fluorescence signal was fitted to a monoexponential decay (bold line).

Being able to trap a single E. coli for an extended time period allowed us to simultaneously observe the photobleaching process of the labeled DNA. The fluorescence signal and the corresponding z-trajectory are shown in Fig. 3c. Up to about 20 s, the trapping remains stable (constant z-position) while the fluorescence signal gradually drops towards the background level of 7 kcps caused by residual waveguide luminescence. Eventually, the fluorescence signal is too low to generate the correct restoring signal to compensate against drift, and the E. coli finally escapes from the trap (see also movie S3 in the ESI).† The fluorescence dynamics were fitted with a mono-exponential decay which yields a bleaching rate of 0.23/s. Such photobleaching studies can be used to study intercellular molecular exchange processes and molecular mobility.[9]

The observed stability limit of about 1 kcps with a signal-to-background ratio of 1 : 3 can be improved by the configuration of the feedback circuitry to the single-photon mode. With this knowledge, both staining density and excitation power can be adjusted to the desired retention time, while lowering the risk of any possible interference from the fluorescent modification with the viable functions of the bacterium.

Improvements to trap scaling properties

To this point, we have described the salient properties of the integrated electro-optical trap: ultralow optical excitation power, single-particle trapping, and ability to simultaneously carry out optical studies on trapped bioparticles in planar beam geometry. The scaling properties of the trap for stability, particle size, and index contrast can be further improved by better confinement in the x- and y-directions. The x-histogram in Fig. 2b shows that the particle samples the entire cross-section of the waveguide and occasionally approaches the channel walls in x. The same applies to the y-direction. At these points, the position of the particle can no longer be tracked due to the vanishing fluorescence collection efficiency (see ESI† for details). Thus, the particle can escape from the trapping region by diffusion or any residual pressure- or voltage-induced motion. This escape mechanism can be mitigated with a variety of integrated approaches. These include local, lithographically defined physical constrictions of the

waveguide in the trapping region, or the construction of additional solid waveguides to provide sensing capabilities in x and y. A simple way of demonstrating the effects of tighter x-y confinement on the trap performance with the present chip geometry is adding an additional guiding beam along the liquid waveguide (see Fig. 1a). In this case, the optical gradient forces confine the particle to the center of the waveguide cross-section and region of maximum detectivity. We conducted several experiments using an infrared guiding beam at 820 nm. This wavelength was chosen to avoid interference with the tracking signal. The effects on the trap can be observed in a number of ways. For example, microbeads subjected to a guiding beam of ~8 mW power (estimated at the particle location) now remain trapped for an unlimited amount of time with improved z-confinement (±80 nm) and are only released by turning off the feedback. In this case, the trap stiffness ($k_z \approx 510$ nN/m) is comparable to conventional optical tweezers where force constants on the order of μN/m are achieved with much higher power (tens of milliwatts).[22]

A second example involves the trapping of nanoscale beads. Fig. 4a shows the z and x-histograms of nanobeads with 200 nm diameter (guiding beam power ≈ 33 mW), *i.e.* a particle volume reduction of more than two orders of magnitude. *Z*-confinement to less than ±0.5 μm and typical trapping times of 10–20 s were achieved. In addition, the fact that the nanobeads sampled the entire waveguide width along x was used to investigate the lateral fluorescence detectivity profile of the waveguide (for details see ESI†). A final example is the improvement for bioparticle studies. In the presence of the guiding beam (27 mW), single E. colis were trapped for 50 s and confined within ±0.5 μm along the fluidic channel. The corresponding photobleaching process is shown in Fig. 4b and shows a reduced bleaching rate of 0.15/s due to the lower fluorescence excitation power used in this experiment. We reiterate that these improvements can also be achieved by a modified sample layout, by using different waveguide materials with lower background luminescence, or by lowering waveguide loss to increase the fluorescence collection efficiency.

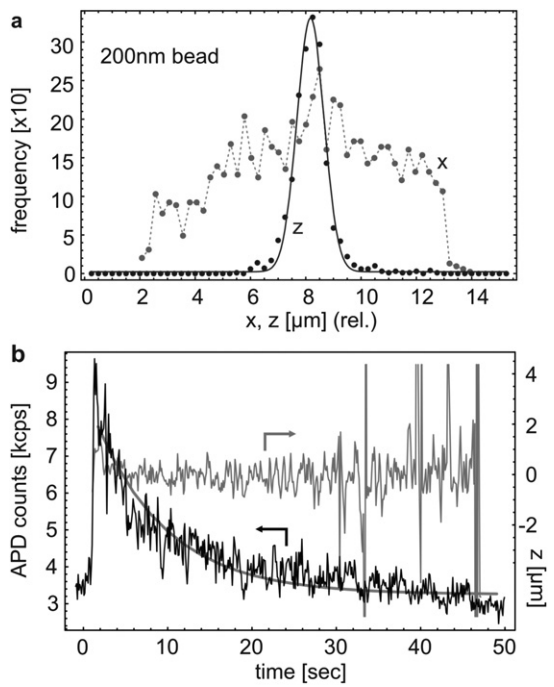

Fig. 4 (a) x and z position histograms for trapped 200 nm fluorescent particles. (b) Time traces of the APD count rate and the z position of an E. coli bacterium during gradual photobleaching. The APD count rate was fitted to a decaying exponential (bold line).

Conclusions

We have described a fully planar, waveguide based particle trap that uses active feedback to eliminate the essential shortcomings of current on-chip optical force traps with the help of active electro-optical trapping. Single micro- and nanoscale objects were confined on an integrated optofluidic chip for extended periods of time with optical excitation powers far below those used in optical force microfluidic traps. The trap overcomes Brownian motion and residual liquid flow. Therefore, it is possible to not only detect the presence of particles but to collect additional information on internal processes like cell division rates, protein expression, viral infection, binding, replication and other biological functions without risking damage to the particle. The technique naturally conforms with the requirements of standard high sensitivity optical analysis methods like FCS and readily allows for thermal and chemical manipulation. While the modulation of the excitation light does not interfere with the observation of processes that occur at slower rates, different excitation wavelengths can be used to study faster dynamics under steady excitation.

This integrated electro-optical trap is clearly suitable for a large class of experiments in molecular biology in which microorganisms or molecules attached to microbeads[23] are studied. In addition, since the ARROW platform can provide single molecule detection sensitivity[24] and the electro-optical trap scales favorably with particle size,[25] it can potentially be used to trap and study individual molecules and biological nanoparticles. This combination of trapping and fluorescence studies of single molecules is extremely challenging to accomplish with conventional optical traps and requires highly optimized setups with numerous limitations and constraints.[26] The active optofluidic electro-optical trap has the potential to reach this regime in a convenient on-chip setting that is extremely simple to operate.

Acknowledgements

We thank P. Measor for his contribution to the taper design for the ARROW waveguide mode filter and D. W. Deamer for support with the culturing and staining of E. coli bacteria. This work was supported by the NIH/NIBIB under grants R01EB006097 and R21EB008802, the NSF under grants ECS-0528730 and ECS-0528714, and the W. M. Keck Center for Nanoscale Optofluidics at UCSC.

Notes and references

1 A. Ashkin, *Phys. Rev. Lett.*, 1970, **24**, 156.
2 A. Ashkin, J. M. Dziedzic, J. E. Bjorkholm and S. Chu, *Opt. Lett.*, 1986, **11**, 288.
3 K. C. Neuman, E. H. Chadd, G. F. Liou, K. Bergman and S. M. Block, *Biophys. J.*, 1999, **77**, 2856.

4 A. Grigorenko, N. Roberts, M. Dickinson and Y. Zhang, *Nat. Photonics*, 2008, **2**, 365.
5 P. Y. Chiou, A. T. Ohta and M. C. Wu, *Nature*, 2005, **436**, 370.
6 J. Enderlein, *Appl. Phys. B: Lasers Opt.*, 2000, **71**, 773.
7 R. S. Decca, C.-W. Lee, S. Lall and S. R. Wassall, *Rev. Sci. Instrum.*, 2002, **73**, 2675.
8 A. E. Cohen and W. E. Moerner, *Proc. Natl. Acad. Sci. U. S. A.*, 2006, **103**, 4362.
9 A. Berglund and H. Mabuchi, *Opt. Express*, 2005, **13**, 8069.
10 S. Cran-McGreehin, T. F. Krauss and K. Dholakia, *Lab Chip*, 2006, **6**, 1122.
11 A. H. J. Yang, S. D. Moore, B. S. Schmidt, M. Klug, M. Lipson and D. Erickson, *Nature*, 2009, **457**, 71.
12 S. Kuehn, P. Measor, B. S. Phillips, D. W. Deamer, A. R. Hawkins and H. Schmidt, *Lab Chip*, 2009, **9**, 2212.
13 H. Schmidt and A. Hawkins, *Microfluid. Nanofluid.*, 2008, **4**, 3.
14 A. Hawkins and H. Schmidt, *Microfluid. Nanofluid.*, 2008, **4**, 17.
15 H. Siefart, *Appl. Opt.*, 1977, **16**, 1163.
16 A. E. Cohen, *Phys. Rev. Lett.*, 2005, **94**, 118102.
17 B. S. Schmidt, A. H. Yang, D. Erickson and M. Lipson, *Opt. Express*, 2007, **15**, 14322.
18 K. C. Neuman and S. M. Block, *Rev. Sci. Instrum.*, 2004, **75**, 2787.
19 D. Magde, E. Elson and W. W. Webb, *Phys. Rev. Lett.*, 1972, **29**, 705.
20 A. J. Berglund, K. McHale and H. Mabuchi, *Opt. Express*, 2007, **15**, 7752.
21 A. Cohen, *Trapping and manipulating single molecules in solution*, Ph.D. thesis, Stanford University (2006).
22 A. Rohrbach and E. H. K. Stelzer, *Appl. Opt.*, 2002, **41**, 2494.
23 C. L. Kuyper and D. T. Chiu, *Appl. Spectrosc.*, 2002, **56**, 300A.
24 D. Yin, D. W. Deamer, H. Schmidt, J. P. Barber and A. R. Hawkins, *Opt. Lett.*, 2006, **31**, 2136.
25 A. E. Cohen and W. E. Moerner, *Opt. Express*, 2008, **16**, 6941.
26 M. Lang, P. Fordyce, A. Engh, K. Neuman and S. Block, *Nat. Methods*, 2004, **1**, 133–139.

